

<sup>2</sup>Miura, K., Furuya, H., and Suzuki, K., "Variable Geometry Truss and Its Application to Deployable Truss and Space Crane Arm," *Acta Astronautica*, Vol. 12, No. 7/8, 1985, pp. 599–607.

<sup>3</sup>Paul, R. P., *Robot Manipulators: Mathematics, Programming, and Control*, MIT Press, Cambridge, MA, 1981, Chap. 2, pp. 41–63.

<sup>4</sup>Tanaka, M., Seguchi, Y., and Hanahara, K., "Kinematics of Adaptive Truss Permitting Nodal Offset (Configuration and Workspace Reach)," *Journal of Intelligent Material Systems and Structures*, Vol. 2, No. 3, 1991, pp. 301–327.

<sup>5</sup>Rao, C. R., and Mitra, S. K., *Generalized Inverse of Matrices and Its Applications*, Wiley, New York, 1971, Chap. 3, pp. 44–71.

A. M. Baz  
Associate Editor

## Modal Actuator/Sensor by Modulating Thickness of Piezoelectric Layers for Smart Plates

Dongchang Sun\* and Liyong Tong†

University of Sydney,

Sydney, New South Wales 2006, Australia

and

Dajun Wang‡

Peking University,

100871 Beijing, People's Republic of China

### I. Introduction

SMART structures with integrated distributed piezoelectric sensors and actuators have been extensively studied in recent years for their potential versatile applications in many aspects, such as aeronautical and astronautical engineering. The independent modal space control (IMSC),<sup>1</sup> which cannot be realized perfectly with the discrete sensors and actuators, can be implemented by the modal sensors and modal actuators with little observation and control spillover by using distributed piezoelectric wafers.<sup>2–7</sup> However, the modal actuators/sensors,<sup>2–4</sup> which are designed by shaping the electric pattern of the piezoelectric layers, are difficult to apply to two-dimensional structures, such as plates and shells, except some special cases. Although the distributed piezoelectric segment method<sup>6,7</sup> can be used for modal control of plates, it can lead to higher costs to control multiple modes simultaneously at a satisfied accuracy. Recently, Tzou et al.<sup>8</sup> gave generic ideas called "spatial thickness shaping" and "spatial surface shaping" to design the modal sensor for shell structures. However, all of their works are concentrated on the spatial surface method without discussing the spatial thickness shaping of the sensor layer.

In this Note, a new practical method is presented to design the modal sensors/actuators by means of modulating the thickness of the piezoelectric wafers. The modal actuators/sensors are designed to excite/sense the designated one or more modes by shaping the thickness of one piezoelectric layer. A simple control scheme is given to perform active control of the smart plates by a modal actuator and

a modal sensor. The control energy can be made to be properly distributed on the dominant modes of the plate by the modal actuator and modal sensor, and, therefore, more effective control results can be achieved. Finally, two approaches are given for implementing the modal sensor/actuator approximately.

### II. Basic Equations for the Piezoelectric Smart Plates

Consider the transverse vibration of a thin plate, on both surfaces of which two piezoelectric layers bonded as the distributed sensor and actuator, as shown in Fig. 1. Assume that the piezoelectric layers are much thinner than the host plate and they are perfectly bonded and that the bonding layers are so thin that their effects on the whole plate can be neglected.

The charge output of the sensor layer can be derived as

$$q(t) = - \iint_S F_s(x, y) \left( \frac{\partial^2 w}{\partial x^2} + \frac{\partial^2 w}{\partial y^2} \right) dx dy \quad (1)$$

where  $q(t)$  is the charge output generated by the piezoelectric sensor layer,  $w(x, y, t)$  is the transverse displacement of the smart plate,  $S$  is the area covered by the sensor layer, and  $F_s(x, y) = e_{31}^s(x, y)r_s(x, y)$  is the spatial distribution function of the sensor layer in which  $e_{31}^s(x, y)$  is the piezoelectric stress coefficient,  $r_s(x, y)$  stands for the  $z$  coordinate of the midplane of the sensor layer from the neutral plane of the smart plate, that is,  $r_s(x, y) = (z_0 + z_1)/2$  and  $z_0, z_1, z_2$ , and  $z_3$  are  $z$  coordinates as shown in Fig. 1.

The differential equation of motion of the smart plate can be derived as

$$\rho h \frac{\partial^2 w}{\partial t^2} + \nabla^2 (D \nabla^2 w) = - \nabla^2 [F_a(x, y) V(x, y, t)] \quad (2)$$

where  $\rho h$  is the equivalent mass density in unit area of the plate,  $D(x, y)$  is the equivalent bending stiffness of the plate,  $V$  is the control voltage, and  $F_a(x, y) = e_{31}^a(x, y)r_a(x, y)$  is the spatial distribution function of the actuator layer. Again,  $e_{31}^a(x, y)$  is the piezoelectric stress coefficient, and  $r_a(x, y) = (z_2 + z_3)/2$  is the  $z$  coordinate of the midplane of the actuator layer.

### III. Modal Actuator Design

Consider the case that the voltage applied on the actuator layer is distributed uniformly in space. In this case the control voltage is only a time-dependent function, that is,  $V(x, y, t) = V(t)$ . The transverse displacement  $w(x, y, t)$  can be expressed as a linear superposition of the modes of the plate, that is,

$$w(x, y, t) = \sum_{i=1}^{\infty} \sum_{j=1}^{\infty} \eta_{ij}(t) W_{ij}(x, y) \quad (3)$$

where  $\eta_{ij}(t)$  and  $W_{ij}(x, y)$  are the  $i, j$ th modal coordinates and modal shape function. Substituting Eq. (3) into Eq. (2), we have

$$\ddot{\eta}_{ij}(t) + \omega_{ij}^2 \eta_{ij}(t) = -V(t) \iint_S \nabla^2 [F_a(x, y)] W_{ij}(x, y) dx dy \quad (4)$$

$i, j = 1, 2, \dots, \infty$

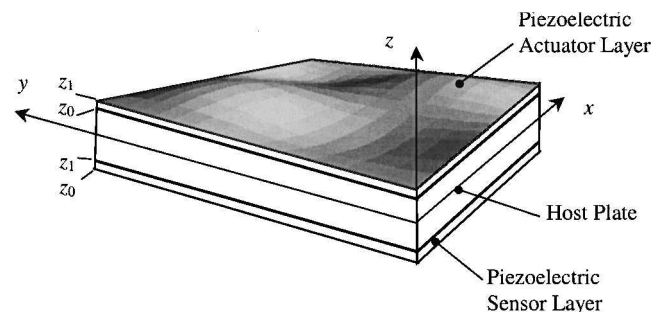


Fig. 1 Plate with piezoelectric sensor and actuator layer.

Received 8 November 1999; revision received 20 April 2001; accepted for publication 17 July 2001. Copyright © 2002 by the American Institute of Aeronautics and Astronautics, Inc. All rights reserved. Copies of this paper may be made for personal or internal use, on condition that the copier pay the \$10.00 per-copy fee to the Copyright Clearance Center, Inc., 222 Rosewood Drive, Danvers, MA 01923; include the code 0001-1452/02 \$10.00 in correspondence with the CCC.

\*Research Associate, School of Aerospace, Mechanical and Mechatronic Engineering; on leave, Associate Professor, School of Mechanical Engineering, Hebei University of Technology, Tianjin 300130, People's Republic of China.

†Associate Professor, School of Aerospace, Mechanical and Mechatronic Engineering. Senior Member AIAA.

‡Professor, Department of Mechanics and Engineering Science.

If only several ( $K \times L$ ) modes of the plate are expected to be excited by the actuator layer, the spatial distribution function should be designed as

$$F_a(x, y) = A_a D \sum_{k=1}^K \sum_{l=1}^L A_{kl}^a \nabla^2 W_{kl}(x, y) + C_a \quad (5)$$

where  $A_{kl}^a$ ,  $A_a$ , and  $C_a$  are constants. Substituting Eq. (5) into Eq. (4), we have

$$\ddot{\eta}_{ij}(t) + \omega_{ij}^2 \eta_{ij}(t) = \begin{cases} -A_a A_{ij}^a \omega_{ij}^2 V(t), & i \leq K, j \leq L \\ 0, & \text{otherwise} \end{cases} \quad (6)$$

which shows that only the selected modes can be excited and other modes are not affected by the actuator layer with spatial distribution function designed in Eq. (5). Therefore, the actuator layer with the designated distribution function becomes a modal actuator.

A feasible method to realize the modal actuator is to modulate the  $z$  coordinate of the midplane of the actuator layer by changing its thickness and keeping the piezoelectric stress coefficient as a constant. In this case the  $z$  coordinate of the midplane of the actuator layer can be determined as

$$\begin{aligned} r_a(x, y) &= \frac{1}{e_{31}^a} F_a(x, y) \\ &= \frac{1}{e_{31}^a} \left[ A_a D \sum_{k=1}^K \sum_{l=1}^L A_{kl}^a \nabla^2 W_{kl}(x, y) + C_a \right] \end{aligned} \quad (7)$$

where  $e_{31}^a$  is the piezoelectric stress constant. Noting that the relation between the  $z$  coordinate of the midplane of the actuator layer and its thickness is  $r_a(x, y) = [z_2 + (z_2 + h_a)]/2$ , the thickness of the modal actuator can be obtained from Eq. (7) as

$$h_a(x, y) = \frac{2}{e_{31}^a} \left[ A_a D \sum_{k=1}^K \sum_{l=1}^L A_{kl}^a \nabla^2 W_{kl}(x, y) + C_a \right] - 2z_2(x, y) \quad (8)$$

To ensure positive thickness of the actuator layer everywhere so that its polarity does not need to be changed, the constants  $A_a$  and  $C_a$  in Eq. (5) should be selected properly. In fact,  $A_a$  controls the undulate degree of the actuator layer, and  $C_a$  is used to keep  $h_a(x, y)$  positive everywhere.

#### IV. Modal Sensor Design

To design the modal sensor, employing Green's formula for Eq. (1) and noting Eq. (3), we have

$$\begin{aligned} q(t) &= - \sum_{i=1}^{\infty} \sum_{j=1}^{\infty} \eta_{ij} \left[ \iint_S W_{ij} \nabla^2 F_s \, dx \, dy \right. \\ &\quad \left. + \int_{\Gamma} W_{ij} \frac{\partial F_s}{\partial n} \, d\Gamma - \int_{\Gamma} F_s \frac{\partial W_{ij}}{\partial n} \, d\Gamma \right] \end{aligned} \quad (9)$$

If the spatial distribution function of the sensor layer satisfies

$$\begin{aligned} F_s(x, y) &= A_s D \sum_{k=1}^K \sum_{l=1}^L A_{kl}^s \nabla^2 W_{kl}(x, y) + C_s, \quad x, y \in S \\ F_s &= 0, \quad \frac{\partial F_s}{\partial n} = 0, \quad x, y \in \Gamma \end{aligned} \quad (10)$$

the following equations can be obtained:

$$q(t) = -A_s \sum_{k=1}^K \sum_{l=1}^L A_{kl}^s \omega_{kl}^2 \eta_{kl}(t) \quad (11)$$

$$I(t) = -A_s \sum_{k=1}^K \sum_{l=1}^L A_{kl}^s \omega_{kl}^2 \dot{\eta}_{kl}(t) \quad (12)$$

where  $I(t)$  is the current output of the sensor,  $A_s$  and  $C_s$  are constants. Equations (11) and (12) show that the sensor layer with the

distribution function satisfying Eq. (10) is only sensitive to the selected modes, and, therefore, such a piezoelectric sensor layer becomes a modal sensor. After obtaining the spatial distribution of the sensor layer from Eq. (10), its thickness distribution function can be determined by following the similar procedure with the actuator. In fact, if the plate is clamped along its four sides the boundary condition in Eq. (10) can be ignored. For a simply supported plate the second boundary condition can be ignored too, and the first boundary condition can be satisfied by choosing  $C_s = 0$ . In this case, to keep the thickness positive, the polarity direction of the parts with negative thickness should be reversed.

#### V. Control Scheme

If  $N$  modal actuator/sensor pairs are designed,  $N$  modes can be controlled independently. However, using one modal actuator/sensor pair, we can control several modes simultaneously (not independently) without affecting the residual modes completely. To control the modes  $\eta_{ij}(t)$  ( $i = 1, 2, \dots, K, j = 1, 2, \dots, L$ ), the control voltage applied on the actuator layer can be simply designed as

$$V(t) = -hI(t) \quad (13)$$

where  $h$  is the control gain. Substituting Eq. (13) into Eq. (6) yields

$$\ddot{\eta}_{ij}(t) + \omega_{ij}^2 \eta_{ij}(t) = h A_a A_{ij}^a \omega_{ij}^2 I(t), \quad i \leq K, j \leq L \quad (14)$$

Inserting Eq. (12) into Eq. (14), the closed-loop equations of the controlled  $N$  modes can be obtained as

$$\ddot{\eta}_{ij}(t) + \sum_{k=1}^K \sum_{l=1}^L C_{ijkl} \dot{\eta}_{kl}(t) + \omega_{ij}^2 \eta_{ij}(t) = 0, \quad i \leq K, j \leq L \quad (15)$$

where  $C_{ijkl} = h A_a A_s A_{ij}^a A_{kl}^s \omega_{ij}^2 \omega_{kl}^2$  are the active damping ratios. If the  $A_{kl}^s$ ,  $A_{kl}^a$ , and  $h$  are selected properly so that all of the eigenvalues have negative parts, the closed-loop system is then stable. Moreover,  $h$  should be also selected to guarantee that the actuator is not depolarized by the control voltage particularly for the region with thinner thickness. The multiple modal control just described is not IMSC. However, all of the control energy is used to control the desired modes without spilling over the residual modes.

#### VI. Approximate Implementation of Modal Actuator/Sensor

To implement the modal actuator/sensor approximately in practice, a natural way is to replace the actuator layer with nonuniform thickness by many small segments with uniform thickness.

One method is to determine thickness of each small segment directly from the thickness distribution of the modal actuator given in Eq. (5). If the actuator layer is divided into  $N_a$  continuous small pieces, the zone covered by the  $n$ th is denoted by  $S_n$ , and the total area of this zone is denoted by  $A_n$ ; the thickness of the  $n$ th segment is simply taken as its average thickness given by

$$h_{an} = \frac{1}{A_n} \iint_{S_n} h_a(x, y) \, dx \, dy, \quad n = 1, 2, \dots, N_a \quad (16)$$

Similarly, the modal sensor can also be implemented approximately following the same procedure. When using the preceding approximate method to design the modal actuator and modal sensor, the control spillover and observation spillover can occur.

Another method to determine the thickness of each actuator segment is based on solving a set of equations rather than the thickness distribution of the modal actuator. Cut the piezoelectric actuator layer into  $M_a \times N_a$  small segments, and each actuator segment  $S_{mn}$  ( $m = 1, 2, \dots, M_a; n = 1, 2, \dots, N_a$ ) has a uniform thickness  $h_{amn}$ . In this case the whole spatial distribution function can be expressed as

$$\begin{aligned} F_a(x, y) &= \sum_{m=1}^{M_a} \sum_{n=1}^{N_a} e_{31}^a r_{amn} [H(x - x_{m-1}) - H(x - x_m)] \\ &\quad \times [H(y - y_{n-1}) - H(y - y_n)] \end{aligned} \quad (17)$$

where  $H(\cdot)$  is the Heavside function. Substituting Eq. (17) into Eq. (4) yields

$$\ddot{\eta}_{ij}(t) + \omega_{ij}^2 \eta_{ij}(t) = V(t) \sum_{m=1}^{M_a} \sum_{n=1}^{N_a} \alpha_{ijmn} r_{amn} \quad i, j = 1, 2, \dots, \infty \quad (18)$$

where  $\alpha_{ijmn}$  are coefficients determined by the location of each segment and the modal function. Making truncation and only the lowest  $M_a \times N_a$  modes being reserved in Eq. (18), Eq. (18) becomes

$$\{\ddot{\eta}(t)\} + [\Omega^2]\{\eta(t)\} = [\hat{A}_a]\{r_a\}V(t) \quad (19)$$

where  $[\Omega^2]$  is a diagonal matrix containing the first  $M_a \cdot N_a$  frequencies of the smart plate,  $\{r_a\} \in R^{M_a \cdot N_a}$  is a vector composed of the  $z$  coordinates of the midplane of the actuator segments, and  $[\hat{A}_a]$  is a  $M_a N_a \times M_a N_a$  square matrix with the entries  $\alpha_{ijmn}$ . If the lowest  $M_a \cdot N_a$  modal forces of the smart plate are designated as  $\{f_a\}V(t)$  similar to Eq. (6),  $\{r_a\}$  can be obtained by solving the algebraic equations

$$[\hat{A}_a]\{r_a\} = \{f_a\} \quad (20)$$

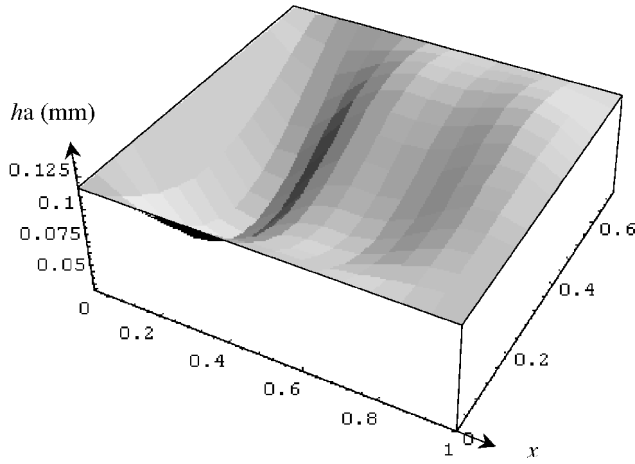
and therefore the thickness of each actuator segment can be easily determined from  $\{r_a\}$ . According to this method, the modal forces for lowest  $M_a \cdot N_a$  are exactly the ones we expected, and the control spillover occurs only in the modes higher than  $M_a \cdot N_a$ .

To realize the modal sensor approximately, cut the piezoelectric actuator layer into  $M_s \times N_s$  small segments, and each actuator segment  $S_{mn}$  has a uniform thickness  $h_{smn}$ . In this case the sensor equation (1) becomes

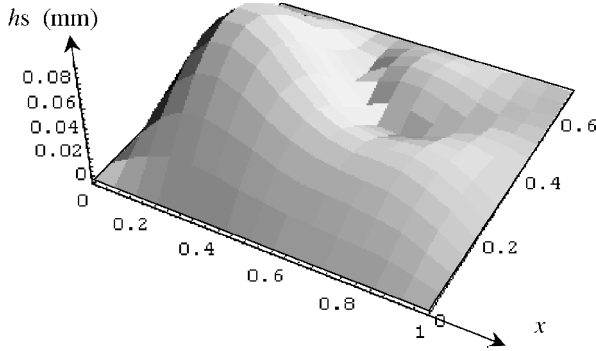
$$q(t) = -e_{31}^s \sum_{m=1}^{M_s} \sum_{n=1}^{N_s} r_{smn} \sum_{i=1}^{\infty} \sum_{j=1}^{\infty} \eta_{ij}(t) \iint_{S_{mn}} \nabla^2 W_{ij}(x, y) dx dy \quad (21)$$

Denoting

$$\beta_{ijmn} = -e_{31}^s \iint_{S_{mn}} \nabla^2 W_{ij}(x, y) dx dy$$



a) Piezoelectric modal actuator



b) Piezoelectric modal sensor

Fig. 2 Thickness distributions of modal actuator/sensor for a simply supported plate.

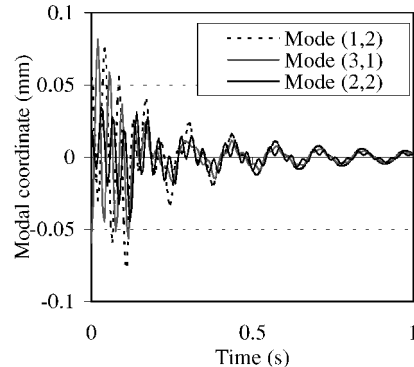
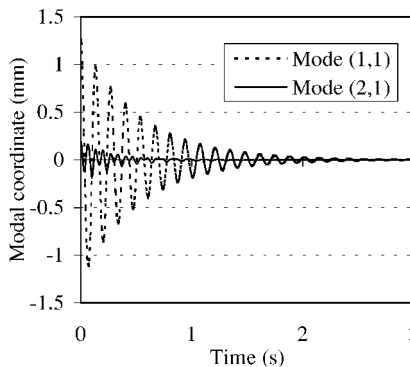
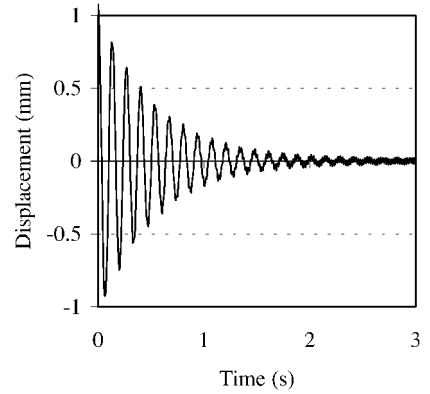
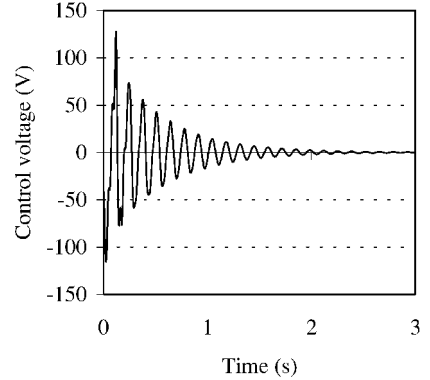


Fig. 3 Five controlled modes of the smart plate.



a) Central displacement



b) Control voltage

Fig. 4 Time history of the central displacement and control voltage.

Eq. (21) can be rewritten as

$$q(t) = \sum_{i=1}^{\infty} \sum_{j=1}^{\infty} \left( \sum_{m=1}^{M_s} \sum_{n=1}^{N_s} \beta_{ijmn} r_{smn} \right) \eta_{ij}(t) \quad (22)$$

Designating the expected weighting coefficient in Eq. (22) as  $p_{ij}$  for the lowest  $M_s \cdot N_s$ , the  $z$  coordinate of the midplane for each sensor segment can be obtained by solving

$$\sum_{m=1}^{M_s} \sum_{n=1}^{N_s} \beta_{ijmn} r_{smn} = p_{ij} \quad i = 1, 2, \dots, M_s, \quad j = 1, 2, \dots, N_s \quad (23)$$

If some modes in the lowest  $M_s \cdot N_s$  modes are not expected to be sensed, the related weighting coefficients are set to be 0. The charge output of the modal sensor might contain the information of the modes whose orders are higher than  $M_s \cdot N_s$ . However, these high-frequency components in the sensed signal can be easily removed by a low-pass filter.

## VII. Results

As an illustrative example, consider a  $1 \text{ m} \times 0.7 \text{ m} \times 1 \text{ mm}$  simply supported rectangular plate onto which one piezoceramic actuator layer and one piezoceramic sensor are bonded. The actuator and the sensor layers are made of the same lead zirconate titanate (PZT) material, and  $e_{31}^a = e_{31}^s = 23.31 \text{ N/Vm}$ . The Young's modulus of the host plate is  $210 \text{ GPa}$ , and its mass density is  $8000 \text{ kg/m}^3$ . The first five (11, 21, 12, 31, 22) modes are selected to be controlled by using the modal sensor and the modal actuator. For the modal actuator the constants in Eq. (5) are taken as  $A_{11}^a = 1.0$ ,  $A_{21}^a = 0.8$ ,  $A_{12}^a = 0.7$ ,  $A_{31}^a = 0.6$ ,  $A_{22}^a = 0.5$ ,  $A_a = 2.5 \times 10^{-5}$ , and  $C_a = 0.013$ , respectively. The maximum thickness of the modal actuator is less than  $0.12 \text{ mm}$ , as shown in Fig. 2a. The modal sensor is designed with the parameters  $A_{11}^s = 1.0$ ,  $A_{21}^s = 0.7$ ,  $A_{12}^s = 0.6$ ,  $A_{31}^s = 0.5$ ,  $A_{22}^s = 0.4$ ,  $A_s = 3 \times 10^{-5}$ , and  $C_s = 0$  so that its maximum thickness is less than  $0.1 \text{ mm}$ , as shown in Fig. 2b. The free vibration of the smart plate is caused by the sudden removal of a force of  $3.5 \text{ N}$  acted on the point  $(0.4, 0.3)$ . Using the modal actuator and modal sensor and taking the control gain  $h$  in Eq. (13) as  $7 \times 10^5$ , the modal control is performed, and the five controlled modes are shown in Fig. 3. The time history of the central displacement of the plate and control voltage applied on the modal actuator during control are presented in Figs. 4a and 4b, respectively. The results show that all of the target modes of the smart plate have been effectively controlled.

When a pair of uniform actuator and sensor layer with the uniformly distributed control voltage are used to control the simply supported rectangular plate, only the strict odd (for example, 11, 33, 55, etc.) modes can be controllable.<sup>9,10</sup> Thus, modulating the thickness of the sensor and actuator layer can make the control more effective and hence improve the controllability of the structures.

## VIII. Conclusions

A new practical method to design the modal actuator/sensor is given for modal control of smart plates by modulating the thickness distribution of the piezoelectric layer. If the stiffness and mass of the piezoelectric layer are considered, the thickness distribution of the modal actuator/sensor can be calculated by an iteration procedure based on a finite element model. In this way the present designing method for modal actuator and modal sensor can be applied to both one-dimensional and two-dimensional structures, such as beams, plates, and shells.

## Acknowledgments

The present work was supported by the Australian Research Council under a Large Research Grant (Grant A89905990) and by the National Science Foundation of China (Grant 19802016, 60034010).

## References

<sup>1</sup>Meirovitch, L., *Dynamics and Control of Structures*, Wiley-Interscience, New York, 1990.

<sup>2</sup>Lee, C.-K., and Moon, F. C., "Modal Sensors/Actuators," *Journal of Applied Mechanics*, Vol. 57, No. 2, 1990, pp. 434–441.

<sup>3</sup>Gu, Y., Clark, R. L., and Fuller, C. R., "Experiments on Active Control Plate Vibration Using Piezoelectric Actuators and Polyvinylidene Fluoride (PVDF) Modal Sensors," *Journal of Vibration and Acoustics*, Vol. 116, No. 3, 1994, pp. 303–308.

<sup>4</sup>Tzou, H. S., Zhong, J. P., and Hollkamp, J. J., "Spatially Distributed Orthogonal Piezoelectric Shell Actuators Theory and Applications," *Journal of Sound and Vibration*, Vol. 177, No. 3, 1994, pp. 363–378.

<sup>5</sup>Ryou, J.-K., Park, K.-Y., and Kim, S.-J., "Electrode Pattern Design of Piezoelectric Sensors and Actuators Using Genetic Algorithms," *AIAA Journal*, Vol. 36, No. 2, 1998, pp. 227–233.

<sup>6</sup>Sun, D. C., Wang, D. J., and Xu, Z. L., "Distributed Piezoelectric Segment Method for Vibration Control of Smart Beams," *AIAA Journal*, Vol. 35, No. 3, 1997, pp. 583, 584.

<sup>7</sup>Sun, D. C., Wang, D. J., and Xu, Z. L., "Distributed Piezoelectric Element Method for Vibration Control of Smart Plates," *AIAA Journal*, Vol. 37, No. 11, 1999, pp. 1459–1463.

<sup>8</sup>Tzou, H. S., Venkayya, V. B., and Hollkamp, J. J., "Orthogonal Sensing and Control of Continua with Distributed Transducers-Distributed Structural System," *Dynamics and Control of Distributed Systems*, edited by H. S. Tzou and L. A. Bergman, Cambridge Univ. Press, Cambridge, England, U.K., 1998, pp. 304–370.

<sup>9</sup>Hubbard, J. E., and Burke, S. E., "Distributed Transducer Design for Intelligent Structural Components," *Intelligent Structural Systems*, edited by H. S. Tzou and G. L. Anderson, Kluwer Academic, Norwell, MA, 1992, pp. 305–324.

<sup>10</sup>Sun, D. C., Wang, D. J., Li, Y., and Xu, Z. L., "Stability and Controllability Analysis of Piezoelectric Smart Plates," *Progress in Natural Science*, Vol. 9, No. 6, 1999, pp. 463–471.

A. M. Baz  
Associate Editor

# Prediction and Design of Metal Plate Vibration Behavior with Bonded Composite Sheets

M. Sasajima,\* T. Kakudate,\* and Y. Narita†  
Hokkaido Institute of Technology,  
Sapporo 006-8585, Japan

## I. Introduction

IN practical situations, structural engineers sometimes face the necessity of increasing the stiffness of already existing structures when applied load in actual use exceeds expected design values or the safety standard is strengthened. One recently emerging technique is to bond composite material sheets externally to the existing structures.<sup>1,2</sup> This technique is now widely used in civil engineering structures by making use of its low cost and ease of operation. The authors found in their experiment that this technique is equally applicable to increase static stiffness and strength of metal plates. This reinforcement was effectively made possible to aluminum plates by epoxy adhesive, and the beam under bending showed relatively large deformation without visible debonding of the sheet.

The present Note studies applicability of this technique to designing the maximum natural frequency of metal (aluminum) plates. Theoretically this problem is more complicated than the static optimization, for example, minimizing static deflection, where increase in the bending stiffness is the only consideration. When dynamic

Received 19 July 2001; revision received 1 December 2001; accepted for publication 12 April 2002. Copyright © 2002 by the American Institute of Aeronautics and Astronautics, Inc. All rights reserved. Copies of this paper may be made for personal or internal use, on condition that the copier pay the \$10.00 per-copy fee to the Copyright Clearance Center, Inc., 222 Rosewood Drive, Danvers, MA 01923; include the code 0001-1452/02 \$10.00 in correspondence with the CCC.

\*Graduate Student, Department of Mechanical Engineering, 7-15 Maeda, Teine-ku.

†Professor, Department of Mechanical Engineering, 7-15 Maeda, Teine-ku; narita@hit.ac.jp.